Molecular Determinants of $PI(4,5)P_2$ and $PI(3,4,5)P_3$ Regulation of the Epithelial Na^+ Channel

Oleh Pochynyuk,[1] Qiusheng Tong,[1] Jorge Medina,[1] Alain Vandewalle,[2,3] Alexander Staruschenko,[4] Vladislav Bugaj,[1] and James D. Stockand[1]

[1]University of Texas Health Science Center, Department of Physiology, San Antonio, TX 78229
[2]INSERM U773, Centre de Recherche Biomedicale Bichat-Beaujon, CRB3 Paris F-75018, France
[3]Universite Paris 7, Denis Diderot, site Bichat, Paris F-75018, France
[4]Medical College of Wisconsin, Department of Physiology and Kidney Disease Center, Milwaukee, WI 53226

Phosphatidylinositol 4,5-bisphosphate ($PI(4,5)P_2$) and phosphatidylinositol 3,4,5-trisphosphate ($PI(3,4,5)P_3$) are physiologically important second messengers. These molecules bind effector proteins to modulate activity. Several types of ion channels, including the epithelial Na^+ channel (ENaC), are phosphoinositide effectors capable of directly interacting with these signaling molecules. Little, however, is known of the regions within ENaC and other ion channels important to phosphoinositide binding and modulation. Moreover, the molecular mechanism of this regulation, in many instances, remains obscure. Here, we investigate modulation of ENaC by $PI(3,4,5)P_3$ and $PI(4,5)P_2$ to begin identifying the molecular determinants of this regulation. We identify intracellular regions near the inner membrane interface just following the second transmembrane domains in β- and γ- but not α-ENaC as necessary for $PI(3,4,5)P_2$ but not $PI(4,5)P_2$ modulation. Charge neutralization of conserved basic amino acids within these regions demonstrated that these polar residues are critical to phosphoinositide regulation. Single channel analysis, moreover, reveals that the regions just following the second transmembrane domains in β- and γ-ENaC are critical to $PI(3,4,5)P_3$ augmentation of ENaC open probability, thus, defining mechanism. Unexpectedly, intracellular domains within the extreme N terminus of β- and γ-ENaC were identified as being critical to down-regulation of ENaC activity and P_o in response to depletion of membrane $PI(4,5)P_2$. These regions of the channel played no identifiable role in a $PI(3,4,5)P_3$ response. Again, conserved positive-charged residues within these domains were particularly important, being necessary for exogenous $PI(4,5)P_2$ to increase open probability. We conclude that β and γ subunits bestow phosphoinositide sensitivity to ENaC with distinct regions of the channel being critical to regulation by $PI(3,4,5)P_3$ and $PI(4,5)P_2$. This argues that these phosphoinositides occupy distinct ligand-binding sites within ENaC to modulate open probability.

The Journal of General Physiology

INTRODUCTION

Ion channels play a critical role in cellular function and physiology. As such, they serve as important effectors for many intracellular signaling cascades, including those using phosphatidylinositide second messengers. Phosphoinositides regulate channel activity both indirectly through the actions of intermediary proteins and more directly by acting as ligands interacting specifically with intracellular portions of channel effectors (Hilgemann et al., 2001; Ribalet et al., 2005; Pochynyuk et al., 2007b; Voets and Nilius, 2007). Phosphoinositide binding often results in channel activation through a molecular mechanism involving increases in open probability. This is the case for phosphoinositide regulation of KCNJ, KCNQ, and KCNK family K^+ channels, TRP channels, epithelial Na^+ channel (ENaC), and Ca_v2 channels (Shyng et al., 2000; Dong et al., 2002; Ma et al., 2002; Wu et al., 2002; Du et al., 2004; Gamper et al., 2004; Tong et al., 2004b; Li et al., 2005; Lopes et al., 2005). Binding and direct channel regulation by phosphoinositides is physiologically important for its disruption can lead to disease. This is true for loss of function mutations in Kir2.1, Kir6.2, and KCNQ1 channels resulting in decreased $PI(4,5)P_2$ affinity/sensitivity leading to Andersen-Tawil, Bartter's, and long QT syndromes, as well as congenital hyperinsulinism (Lopes et al., 2002; Donaldson et al., 2003; Park et al., 2005; Lin et al., 2006; Ma et al., 2007). In several instances, disease-causing mutations modify the basic residues involved in forming electrostatic interactions with the negative-charged head groups of phosphoinositides. While diverse types of channels directly bind and, thus, are sensitive to phosphoinositides, details regarding sites within ion channels involved in this regulation and binding remain obscure. Moreover, the molecular consequences of phosphoinositide binding to ion channels, in many cases, remain conjecture.

Correspondence to James D. Stockand: stockand@uthscsa.edu

Abbreviations used in this paper: ENaC, epithelial Na^+ channel; PH, pleckstrin homology; PI3-K, phosphatidylinositide 3-OH kinase; $PI(4,5)P_2$, phosphatidylinositol 4,5-bisphosphate; $PI(3,4,5)P_3$, phosphatidylinositol 3,4,5-trisphosphate; TIRF, total internal reflection fluorescence.

Here, we continue probing phosphoinositide regulation of ENaC to address some of these questions. ENaC is believed to interact with both $PI(4,5)P_2$ and $PI(3,4,5)P_3$ with direct interactions influencing channel activity (Ma et al., 2002; Yue et al., 2002; Tong et al., 2004b; Kunzelmann et al., 2005; Pochynyuk et al., 2005; Tong and Stockand, 2005).

The epithelial Na^+ channel is a nonvoltage-gated, noninactivating, highly Na^+-selective channel localized to the luminal plasma membrane of epithelial cells (Garty and Palmer, 1997; Benos and Stanton, 1999; Alvarez de la Rosa et al., 2000; Kellenberger and Schild, 2002). ENaC is common to a number of different epithelial tissues, including those lining the distal renal nephron, distal colon, ducts of exocrine glands, and pulmonary airways and alveolar sacs. ENaC activity is rate limiting for Na^+ (re)absorption across these epithelial barriers. Because of this function, ENaC serves as a critical modulator of epithelial hydration, setting osmotic gradients driving fluid movement. Moreover, ENaC in the kidneys and colon is positioned to influence systemic Na^+ balance and, thus, blood pressure. Indeed, ENaC is a final effector of the renin-angiotensin–aldosterone system, which is the primary negative feedback pathway governing blood pressure. As such, gain of function mutations in ENaC and its upstream regulatory pathways are causative for several hypertensive diseases associated with improper Na^+ retention (Snyder et al., 1995; Abriel et al., 1999; Hummler and Horisberger, 1999; Bonny and Hummler, 2000; Lifton et al., 2001). Conversely, loss of function mutations in ENaC and its upstream regulatory pathways cause renal salt wasting diseases and the inability to clear the neonatal lung of fluid after birth.

The primary systemic regulators of ENaC are corticosteroids, including mineralocorticoids, such as aldosterone, and glucocorticoids (Verrey, 1995; Verrey, 1999; Stockand, 2002). ENaC also responds to endocrine and paracrine signals like insulin and ATP. Both aldosterone and insulin increase ENaC activity through a transduction cascade including phosphatidylinositide 3-OH kinase (PI3-K) and its product phosphoinositides (Record et al., 1998; Blazer-Yost et al., 1999; Wang et al., 2001; Staruschenko et al., 2004c). Activation of ENaC by PI3-K signaling involves, at least in part, direct interactions of $PI(3,4,5)P_3$ with channel subunits (Tong et al., 2004a,b; Pochynyuk et al., 2005). In contrast to aldosterone and insulin, ATP, most likely via PLC linked to a G_q-coupled receptor, decreases $PI(4,5)P_2$ levels in epithelial cells; consequently, decreasing ENaC activity (Ma et al., 2002; Kunzelmann et al., 2005). Again, this regulation involves direct interaction between the phosphoinositide and channel.

ENaC is a heteromeric channel comprised of three distinct but similar subunits: α, β, and γ (Canessa et al., 1993, 1994). The exact subunit stoichiometry of ENaC remains uncertain; however, all three subunits are required for normal channel activity, regulation, and function (Canessa et al., 1994; McNicholas and Canessa, 1997; Fyfe and Canessa, 1998). Each of these three subunits shares a common tertiary structure having intracellular N and C termini separated from a single large extracellular loop by transmembrane domains (Snyder et al., 1994).

While $PI(3,4,5)P_3$ and $PI(4,5)P_2$ may bind to modulate ENaC activity, little is actually know about putative binding sites for these ligands in this channel (Pochynyuk et al., 2007b). This lack of understanding is not unique to ENaC for little is actually known about putative phosphoinositide binding sites in most phosphoinositide-sensitive ion channels. What we do know comes primarily from study of $PI(4,5)P_2$ binding to Kir and TRP channels (Zhang et al., 1999; Shyng et al., 2000; Soom et al., 2001; Cukras et al., 2002a,b; Dong et al., 2002; Lopes et al., 2002, 2005; Prescott and Julius, 2003; Rohacs et al., 2003; Du et al., 2004).

Channel–phosphoinositide interactions are thought to be primarily electrostatic in nature, where the negative-charged head groups of phosphoinositides interact with positive-charged residues within intracellular portions of the channel. In addition, polar and nonpolar residues, which do not directly interact with the charged phosphates, further stabilize this interaction. Importantly, intracellular regions of ion channels just following transmembrane domains, which often are rich in positive-charged residues, are particularly involved in coordinating phosphoinositide binding (Zhang et al., 1999; Shyng et al., 2000; Soom et al., 2001; Dong et al., 2002; Prescott and Julius, 2003; Bian et al., 2004).

To learn more about the molecular mechanism of phosphoinositide regulation of ENaC and to better understand the domains within ion channels important to phosphoinositide regulation and potentially important to binding, we investigated the effects of $PI(3,4)P_2$ and $PI(3,4,5)P_3$ on ENaC. Substitution mutations, resulting in charge neutralization, and deletions were targeted to intracellular residues/domains having characteristics of phosphoinositide bind sites. We find that intracellular regions of β- and γ- but not α-ENaC are necessary for $PI(4,5)P_2$ and $PI(3,4,5)P_3$ regulation. Unexpectedly, different regions of the channel were necessary to regulation by these two phosphoinositides with the extreme N terminus being involved in regulation by the former and regions just following the second transmembrane domains being important to regulation by the latter. Both phosphoinositides affected ENaC open probability and conserved positive-charged residues played key roles in the response.

MATERIALS AND METHODS

Chemicals and cDNA Constructs

All chemicals were from Sigma-Aldrich, BioMol, or CalBiochem, unless noted otherwise. All materials used in Western blot analysis

were from Bio-Rad Laboratories. Sulfo-NHS-LC-biotin and streptavidin-agarose were from Pierce Chemical Co. The mouse monoclonal anti-myc antibody was from CLONTECH Laboratories, Inc. and the rabbit anti-Fra-2 polyclonal antibody was from Santa Cruz Biotechnology, Inc. Anti-mouse and anti-rabbit HRP-conjugated 2° antibodies were from Kirkegaard-Perry Laboratories. ECL reagents were from PerkinElmer Life Sciences. Dioctanoyl (diC8), short-chain phosphatidylinositides were from Echelon Biosciences Inc. The expression vector encoding membrane-targeted PI3-K (pUSE-amp-p110α) was from Upstate Biotechnology. This plasmid encodes p110α fused to an N-terminal Src myristoylation sequence, which localizes PI3-K to the plasma membrane, where it is then constitutively active (Kristof et al., 2003). The mammalian expression vector encoding type I PI(4)P5-kinase α-isoform was a gift from L. Pott (Ruhr University Bochum, Bochum, Germany) and has been described previously (Bender et al., 2002). The $PI(4,5)P_2$ reporter, GFP-PLC-δ-PH, is a chimera consisting of the $PI(4,5)P_2$-binding pleckstrin homology (PH) domain from PLC-δ conjugated to GFP (Haugh et al., 2000). The cDNA encoding this reporter was a gift from the T. Meyer laboratory (Stanford University, Stanford, CA). The mammalian expression vectors encoding α-, β-, and γ-mouse ENaC with N-terminal myc- and HA-epitope tags have been described previously (Staruschenko et al., 2004c; Tong et al., 2004b; Pochynyuk et al., 2005). As noted in these earlier publications, channels comprised of epitope-tagged subunits exhibit functional behavior indistinguishable from those lacking tags. All ENaC mutagenesis was performed on the backbone of plasmids encoding myc-tagged subunits. Mutants were created in our laboratory with QuikChange (Stratagene) mutagenesis per the manufacture's instructions or outsourced to TOP Gene Technologies. Regardless of source, every plasmid encoding an ENaC subunit mutant was sequenced to ensure proper incorporation of the expected mutation and to confirm sequence identity, orientation, and reading frame. We used 12 mENaC mutants in this study: (1) three of α-ENaC, including the R98-K108 (α1D) and R614-R630 (α2D) deletions and the R98A + K103A (α1S) substitution; (2) four of β-ENaC, including the K4-K16 (βND), K39-K49 (β1D), and K552-R563 (β2D) deletions and the K39A + R40A (β1S) substitution; and (3) five of γ-ENaC, including the R42-R53 (γ1D) and Q573-R583 (γ2D) deletions and the K6A + K8A + K10A + K12A + K13A (γNS), R42A + R43A (γ1S), and R569A + R570A + K574A + K576A + R581A + R582A + R583A (γ2S) substitutions. The relative position of these mutations to the first and second transmembrane domains in ENaC subunits are shown in Fig. 1 A.

Cell Lines and Tissue Culture

CHO cells were from American Type Culture Collection. These cells were maintained with standard culture conditions (DMEM + 10% FBS, 37°C, 5% CO_2) as described previously (Staruschenko et al., 2004c; Tong et al., 2004b; Pochynyuk et al., 2005). Immortalized mouse cortical collecting duct ($mpkCCD_{c14}$) principal cells were grown in defined medium on permeable supports (Costar Transwells; 0.4 μm pore, 24 mm diameter) as described previously (Bens et al., 1999). Cells were maintained with FBS and corticosteroids allowing them to polarize and form monolayers with high resistances and avid Na^+ reabsorption.

Expression of Exogenous Protein

Recombinant ENaC and phospholipid kinases were overexpressed in CHO cells by transfecting the appropriate expression plasmids using the Polyfect reagent (QIAGEN) as described previously (Staruschenko et al., 2004c; Tong et al., 2004b; Pochynyuk et al., 2005). For electrophysiology studies, 0.3 μg/subunit/9.6 cm^2 plasmid cDNA was used. Plasmid cDNAs encoding phospholipid kinases were added at 1.0 μg/9.6 cm^2. For membrane labeling studies, 1.0 μg/subunit/314 cm^2 plasmid cDNA was used. The plasmid encoding the $PI(4,5)P_2$ reporter, GFP-PLC-δ-PH, was introduced into $mpkCCD_{c14}$ principal cells within a confluent monolayer with a biolistic particle delivery system (Biolistic PDS-1000/He Particle Delivery System; Bio-Rad Laboratories). Use of this system has been described previously (Yuan et al., 2005; Gamper and Shapiro, 2006). We closely followed established protocols in the current studies. In brief, $mpkCCD_{c14}$ cells were grown to confluence on permeable supports. After forming high-resistance monolayers avidly transporting Na^+, cells were washed twice with physiologic saline, aspirated, and quickly bombarded (at the apical membrane) under vacuum with microcarriers coated with GFP-PLC-δ-PH cDNA. Medium was immediately returned to the cells, which where then placed within a tissue culture incubator for 2–3 d to allow expression of the $PI(4,5)P_3$ reporter. Bombardment had little disruptive effect on cellular and monolayer integrity as established by maintenance of Na^+ transport and a high transepithelial resistance.

Total Internal Reflection Fluorescence (TIRF) Microscopy

Fluorescence emissions from the $PI(4,5)P_2$ reporter at the apical membrane of $mpkCCD_{c14}$ cells within a confluent monolayer were collected using TIRF (also called evanescent-field) microscopy. TIRF generates an evanescent field that declines exponentially with increasing distance from the interface between the cover glass and plasma membrane, illuminating only a thin section (~100 nm) of the cell in contact with the cover glass (Steyer and Almers, 2001; Axelrod, 2001; Taraska et al., 2003). For these experiments, GFP-PLC-δ-PH was introduced into polarized monolayers of $mpkCCD_{c14}$ cells grown on permeable supports with the particle delivery system described above. Upon expression of the reporter, 5 × 5-mm sections of the support were excised, inverted, and placed onto cover glass coated with poly-L-lysine. This arrangement made it possible to visualize dynamic changes in the level of the $PI(4,5)P_2$ reporter at the apical membrane in real time in living cells.

All TIRF experiments were performed in the total internal reflection fluorescence microscopy core facility housed within the Department of Physiology at the University of Texas Health Science Center (http://physiology.uthscsa.edu/tirf). We have previously described imaging the GFP-PLC-δ-PH reporter and other fluorophore-tagged proteins using this core facility (Tong et al., 2004b; Staruschenko et al., 2005; Pochynyuk et al., 2006a). The methods used in the current study closely followed these published protocols. In brief, fluorescence emissions from GFP-PLC-δ-PH were collected using an inverted TE2000 microscope with through-the-lens (prismless) TIRF imaging (Nikon). Samples were viewed through a plain Apo TIRF 60x oil-immersion, high-resolution (1.45 NA) objective. Fluorescence emissions were collected through a 535 ± 25-nm bandpass filter (Chroma Technology Corp.) by exciting GFP with an Argon-ion laser with an acoustic optic tunable filter (Pairie Technology Inc.) used to restrict excitation wavelength to 488 nm. Fluorescence images were collected and processed with a 16-bit, cooled charge-coupled device camera (Cascade 512F; Roper Scientific Inc.) interfaced to a PC running Metamorph software. This camera uses a front-illuminated EMCCD with on-chip multiplication gain. Images were collected once a minute with a 100-ms exposure time. Images were not binned or filtered with pixel size corresponding to a square of 122 nm × 122 nm.

Membrane Labeling Experiments

Membrane labeling experiments closely followed those described previously (Booth and Stockand, 2003; Staruschenko et al., 2004b,c). In brief, CHO cells were transfected with myc- and HA-tagged ENaC subunits. The subunit of interest contained the myc tag and was followed with anti-myc antibody. 48 h after

transfection, cells were washed three times with ice-cold PBS (pH 8.0) and subsequently incubated with 3 mM sulfo-NHS-LC-biotin (in PBS, pH 8.0) for 30 min at room temperature in the dark. Cells were washed again three times with ice-cold PBS plus 100 mM glycine to quench the reaction and then extracted in gentle lysis buffer (76 mM NaCl, 50 mM HCl-Tris, pH 7.4, 2 mM EGTA, plus 1% Nonidet P-40 and 10% glycerol; supplemented with the protease inhibitor 1 mM phenylmethylsulfonyl fluoride). Extracts were cleared and normalized for total protein concentration. Pre-equilibrated streptavidin agarose beads were agitated overnight at 4°C with 200 μg total protein. Agarose beads were then washed six times with gentle lysis buffer and subsequently resuspended in SDS sample buffer and 20 mM DTT, heated at 85°C for 10 min, run on 7.5% polyacrylamide gels in the presence of SDS, transferred to nitrocellulose, and probed with anti-myc antibody in tris-buffered saline supplemented with 5% dried milk and 0.1% Tween-20. Band intensity in developed blots was quantified by scanning the blots and then using Sigma-Gel (Jandel Scientific) to analyze digital images. We used a flood-above-threshold protocol with threshold set to the highest practical level.

Electrophysiology

Whole-cell macroscopic current recordings of ENaC reconstituted in CHO cells were made under voltage-clamp conditions using standard methods (Staruschenko et al., 2004c; Tong et al., 2004b; Pochynyuk et al., 2005). Current through ENaC was the inward, amiloride-sensitive Na^+ current with a bath solution of (in mM) 160 NaCl, 1 $CaCl_2$, 2 $MgCl_2$, and 10 HEPES (pH 7.4) and a pipette solution of (in mM) 140 CsCl, 5 NaCl, 2 $MgCl_2$, 5 EGTA, 10 HEPES (pH 7.4), 2.0 ATP, and 0.1 GTP. Current recordings were acquired with an Axopatch 200B (Axon Instruments) interfaced via a Digidata 1322A (Axon Instruments) to a PC running the pClamp 9.2 suite of software (Axon Instruments). All currents were filtered at 1 kHz. Voltage ramps (500 ms) from 60 to −100 mV from a holding potential of 40 mV were used to generate current–voltage (I-V) relations and to measure ENaC activity at −80 mV. Whole-cell capacitance was routinely compensated and was ∼9 pF for CHO cells. Series resistances, on average 2–5 MΩ, were also compensated.

For excised, outside-out patches made on CHO cells overexpressing wild-type and mutant ENaC, bath and pipette solutions were (in mM) 160 NaCl, 1 $CaCl_2$, 2 $MgCl_2$, and 10 HEPES (pH 7.4) and 140 CsCl, 5 NaCl, 2 $MgCl_2$, 5 EGTA, 10 HEPES (pH 7.4), 2.0 ATP, and 0.1 GTP (in mM), respectively. Current recordings were made under voltage-clamp conditions using an Axopatch 200B. Currents were low-pass filtered at 100 Hz by an eight-pole Bessel filter (Warner Instruments) and digitized at 500 Hz and stored on a PC using the Digidata 1322A interface. For presentation, some currents were subsequently software filtered at 40 Hz. Gap-free current recordings were made at pipette potentials (V_p) of 0 or −60 mV with inward Na^+ current downwards. Current data were analyzed using pClamp 9.2. Channel activity defined as NP_o was calculated using the following equation: $NP_o = \Sigma(t_1 + 2t_2 + \ldots it_i)$, where t_i is the fractional open time spent at each of the observed current levels. P_o was estimated by normalizing NP_o for the observed number of channels within a patch as established with all-point histograms. The error associated with this estimation of P_o increases as patches contain more channels and as P_o approaches either zero or unity (Kemendy et al., 1992). While there is an error associated with estimating P_o in seals containing more than one channel, it can be lessened, as done here, by restricting this calculation to patches containing only five channels or fewer. Moreover, the error associated with this measurement was further limited by estimating P_o over a span of 35–120 s for each condition. Calculations for channels in excised, inside-out patches were made using the number of channels observed before "rundown." Single channel current–voltage relations were generated from unitary currents defined by all-point histograms at six different holding potentials from, at least, four independent experiments. Aqueous stocks of water-soluble, short-chain diC8 phosphoinositides were prepared at 1 mM by sonication for 30 min and stored at −70°C. Stock phosphoinositides were mixed just before use with an equal volume of a carrier solution containing histone H1 (0.2 mM; Echelon Biosciences Inc.) and sonicated again for 10 min. Phosphoinositide plus carrier was added to the bathing solution by direct pippetting close to the patched membrane.

For cell-attached patches made on the apical membranes of $mpkCCD_{c14}$ principal cells, bath and pipette solutions were (in mM) 160 NaCl, 1 $CaCl_2$, 2 $MgCl_2$, and 10 HEPES (pH 7.4); and 140 LiCl, 2 $MgCl_2$, and 10 HEPES (pH 7.4), respectively. Current recordings were made at a $-V_p = -60$ mV and collected and analyzed as above.

For excised, inside-out patches, bath and pipette solutions were (in mM) 140 CsCl, 0.5 $MgCl_2$, 5 EGTA, and 10 HEPES (pH 7.4); and 140 LiCl, 2 $MgCl_2$, and 10 HEPES (pH 7.4), respectively. Exogenous phosphoinositide was added in the presence of 0.1 mM GTP. Current recordings were made at $-V_p = -60$ mV, and collected and analyzed as above.

Statistics

All summarized data reported as mean ± SEM. Membrane levels of ENaC normalized to total cellular pools. Emissions from GFP-PLC-δ-PH normalized to starting levels. Emissions were corrected for a modest, time-dependent photobleaching (<15%/15 min) as established with vehicle treatment. Macroscopic current density in the presence of PI3-K, PI(4)P5-K, and VO_4 reported relative to control levels. Summarized data compared with either the Student's *t* test or a one-way ANOVA in conjunction with the Dunnett post-test where appropriate. $P \leq 0.05$ was considered significant.

RESULTS

Characterization of ENaC Subunit Mutants

All three ENaC subunits have cytosolic tracks just preceding and following the first (TM1) and second (TM2) transmembrane domains containing clusters of conserved positive-charged residues. In addition, β- and γ-ENaC have clusters of basic residues in their extreme N terminus. We begin our investigation of phosphoinositide regulation of ENaC by characterizing channels containing charge neutralization and deletion of these conserved positive-charged residues. Fig. 1 A notes the relative position of substituted and deleted residues with respect to the transmembrane domains within ENaC.

Fig. 1 B shows results from experiments confirming that each mutant subunit expresses, produces a peptide of the expected size, and localizes to the plasma membrane when coexpressed with complementary wild-type subunits. Typical results for each mutant are shown in the Western blots to the right with summary data compared in the graph to the left. For these experiments, ENaC in the plasma membrane (M) was separated from total cellular pools (T) of the channel. The inset in Fig. 1 B shows a complete Western blot representative of such experiments. The top blot in this inset contains whole cell lysates (T) and membrane fractions (M) from

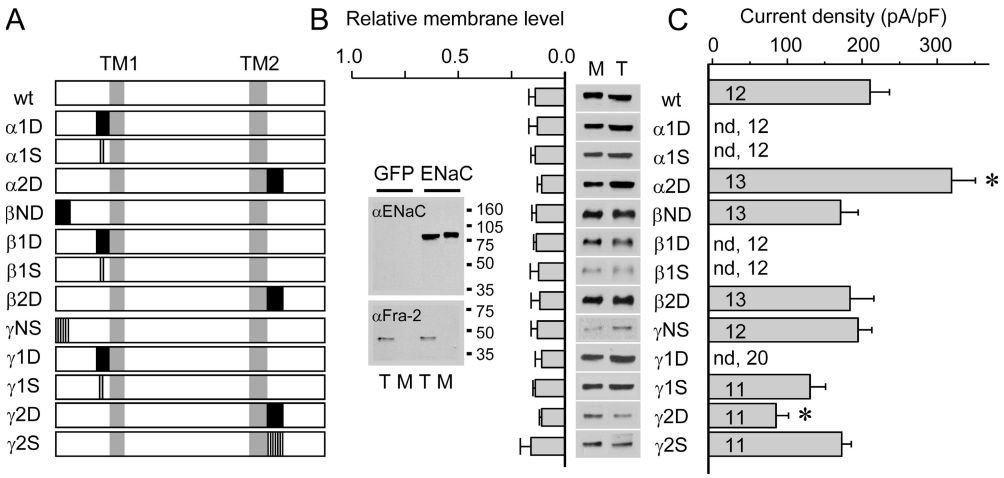

Figure 1. ENaC mutants used to probe phosphoinositide regulation. (A) Schematic representation of wild-type and mutant mENaC subunits. The N and C termini are intracellular and separated by two transmembrane domains (TM1 and TM2; shown as gray boxes) and a large extracellular region. The relative positions of deletion (black boxes) and substitution (black lines) mutations are indicated. (B) Regions of note (between molecular weight markers 75 and 105 kD) from typical Western blots (right) containing whole-cell lysates (T) and membrane fractions (M; isolated from 4x T) from CHO cells expressing wild-type and mutant ENaC. Shown in the inset is a full blot from cells expressing wild-type ENaC and the negative eGFP control. All blots probed with anti-Myc antibody to identify the ENaC subunit of interest (α-ENaC in top blot of inset). Blots were subsequently stripped and counterprobed with anti–Fra-2 (bottom blot of inset) to ensure good separation of M from T. The summary graph to the left reports relative membrane levels. Summary data from three to six experiments for each group. (C) This graph summarizes the activity of recombinant ENaC expressed in CHO cells containing all wild-type (wt) and the respective mutant subunits. Activity quantified in whole-cell voltage clamp experiments as the amiloride-sensitive macroscopic current density at −80 mV. The numbers of observations for each group shown. *, significantly different using a one-way ANOVA plus the Dunnett's subtest comparing treatment groups to the control wild-type group.

CHO cells overexpressing all three wild-type ENaC subunits and from those expressing the negative control, eGFP. This blot first was probed with anti-myc antibody to identify α-ENaC (top) and then stripped and subsequently reprobed with anti–Fra-2 antibody (bottom). The prior antibody identifies the channel subunit of interest and the latter confirms good separation of the membrane fraction from total cellular pools for Fra-2 is a cytosolic protein. In every case, mutant ENaC expressed normally, with mutation having no overt effect on the relative membrane levels of the channel.

We continued characterizing mutant ENaC with whole-cell voltage clamp experiments. Results are shown in Fig. 1 C. As reported previously (Booth et al., 2003; Staruschenko et al., 2004c; Tong et al., 2004b), CHO cells have little background current and no amiloride-sensitive current in the absence of overexpression of ENaC. Coexpression of all three wild-type subunits resulted in an activity of 210 ± 26 pA/pF. In contrast, ENaC-containing subunits with mutations in the regions just preceding TM1 were not active, except for that containing a subtle substitution in this region of γ-ENaC. In contrast, channels comprised of subunits having mutations in their N terminus and just after TM2 were active.

While the region just preceding TM1 in all three subunits appears to be critical for normal channel function, the scope of the current study is to identify regions of ENaC important to phosphatidylinositide regulation. In this context, mutations having little effect on basal activity, such as those following TM2 and those in the N termini of β- and γ-ENaC, are more useful compared with those that result in a complete loss of function.

Conserved Positive-charged Residues in the Cytosolic Regions just following TM2 in β- and γ-ENaC Are Necessary for PI3-K and PI(3,4,5)P_3-sensitive Increases in P_o

We now were positioned to test whether mutant ENaC, as wild-type ENaC, responds to PI3-K stimulation. To do this, mutant subunits were coexpressed with complementary wild-type subunits in the absence and presence of constitutively active PI3-K. Relative increases in activity in the presence of PI3-K measured in whole-cell voltage clamp experiments for wild-type and mutant channels are shown in Fig. 2. Mutation of the region following TM2 in β- and γ-ENaC subunits completely abolished PI3-K sensitivity. In contrast, channels with α subunits containing mutation of this region and those containing β and γ subunits with N-terminal mutations had normal responses to PI3-K. Similarly, channels containing the only functional mutant of the area just preceding TM1, γ1S, had a robust response to coexpression of PI3-K not different than wild type. These results demonstrate that PI3-K increases ENaC activity in a manner dependent on the regions just following TM2 in β- and γ-ENaC. More specifically, the response to PI3-K depends on the presence of conserved positive-charged residues within these regions. This is the first indication that this region of β-ENaC plays an important role in PI3-K regulation. The observation that this region of γ-ENaC plays a role in the response to PI3-K is consistent with the same finding made previously by our laboratory and our finding that this area of γ-ENaC physically interacts with the phosphatidylinositide products of PI3-K, PI(3,4,5)P_3, and PI(3,4)P_2 (Pochynyuk et al., 2005).

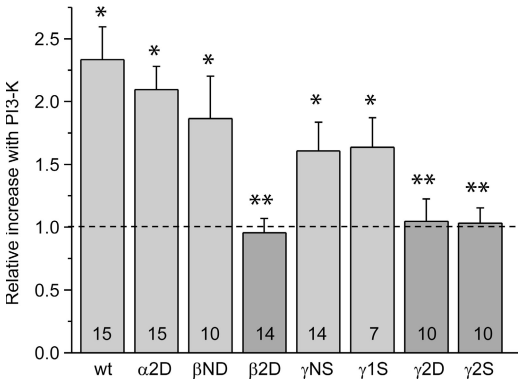

Figure 2. The regions just following TM2 in β- and γ-ENaC subunits are necessary for PI3-K regulation. Summary graph of the relative increase in ENaC activity in the presence of constitutively active PI3-K for wild-type channels and channels containing a single type of mutant subunit coexpressed with complementary wild-type subunits. Activity of recombinant wild-type and mutant ENaC quantified in whole-cell voltage clamp experiments on CHO cells. All conditions the same as in Fig. 1 C. *, significant increase in activity compared with that in the absence of PI3-K. **, significantly different compared with wild type using an ANOVA plus the Dunnett's subtest.

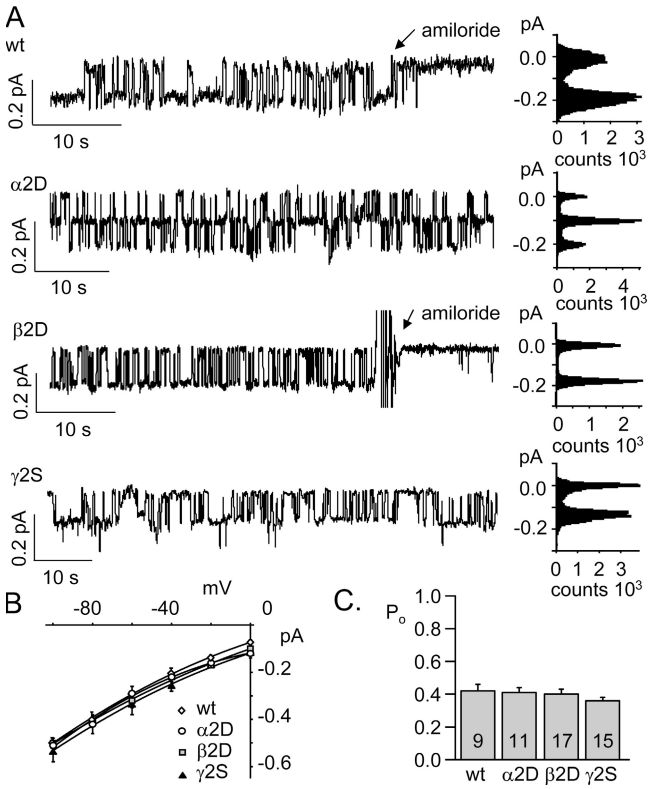

Figure 3. ENaC containing wild-type and mutant subunits used to probe regulation by phosphoinositides are not different at the single channel level in resting CHO cells. (A) Representative current traces (left) and associated all-point histograms (right) from excised, outside-out patches (V_p = 0 mV) made from CHO cells expressing ENaC containing all wild-type subunits (top) and a single mutant subunit coexpressed with complementary wild-type subunits. Inward current is downwards. As shown in the latter portions of the traces from patches containing wild-type and β2D mutant channels, 10 μM amiloride was routinely added to the bathing solution. This was a standard procedure used to confirm that these Na^+-selective, nonvoltage-activated, ~5 pS channels with hallmark slow gating kinetics were indeed recombinant ENaC. Such channels were absent in nontransfected cells. (B) Summary single channel current–voltage relations for wild-type and mutant ENaC. Data is from, at least, four independent excised, outside-out patches for each group. (C) Summary graph of resting P_o for wild-type and mutant ENaC in CHO cells. Summary data is from excised, outside-out patches similar to those in A.

To extend these results to better understand mechanism, we next investigated regulation of ENaC by PI3-K and its products at the single channel level. Fig. 3 A shows current traces (left) and corresponding all-point histograms (right) for ENaC in representative excised, outside-out patches from cells expressing wild-type channels (top) and channels containing either the α2D (top middle), β2D (bottom middle), or γ2S (bottom) mutant subunit. As is clear in these representative traces and reported previously by us (Tong et al., 2004b; Pochynyuk et al., 2005; Tong and Stockand, 2005), ENaC activity is stable under these seal conditions. The representative current traces and histograms, as well as the summary single channel current–voltage (I-V) relations (Fig. 3 B) and open probability (C) graphs demonstrate that there is little difference at rest in the basal activity and unitary conductance of ENaC containing all wild-type subunits and those containing a single type of mutant subunit. All were highly selective for Na^+ over K^+, had single channel conductances at hyperpolarizing potentials ~5 pS with Na^+ as the charge carrier, and had open probabilities approaching 0.4 that were not significantly different. The preference for Na^+ over K^+, and P_o and conductance values agree well with that reported previously for recombinant and native ENaC, and are consistent with the results in Fig. 1 C where channels containing β2D and γ2S mutant subunits had basal activities similar to wild-type channels.

The representative current trace of wild-type mENaC in an excised, outside-out patch in Fig. 4 records a typical response to exogenous $PI(3,4,5)P_3$. As is apparent in the continuous current trace shown at the top, as well as in the current traces and associated all-point histograms shown below at expanded time scales before (1. control) and after (2. PIP_3) addition of exogenous $PI(3,4,5)P_3$, treatment markedly increases channel activity by affecting P_o. This patch contains, at least, five ENaC, which become easy to resolve following the slowing of gating and stabilization of the open state upon addition of $PI(3,4,5)P_3$. This characteristic response to exogenous $PI(3,4,5)P_3$ is consistent with that reported previously for wild-type mENaC (Tong et al., 2004b; Pochynyuk et al., 2005).

Fig. 5 contrasts the effects of exogenous $PI(3,4,5)P_3$ on the P_o of PI3-K responsive (α2D; Fig. 5 A) and unresponsive

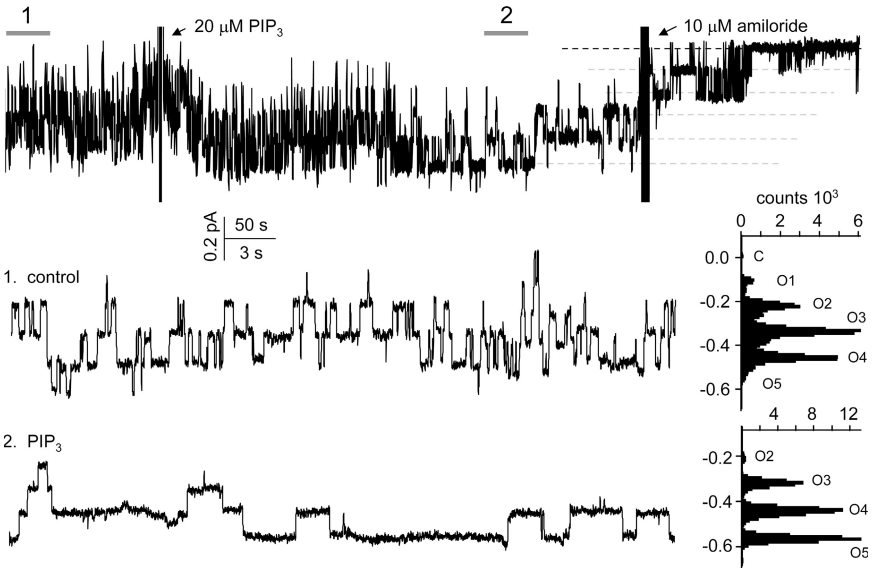

Figure 4. A typical response of ENaC to exogenous $PI(3,4,5)P_3$. Shown is a representative current trace from an excised, outside-out patch (V_p = 0 mV) formed from a CHO cell expressing wild-type ENaC before and after addition of 20 μM exogenous diC8 $PI(3,4,5)P_3$. $PI(3,4,5)P_3$ added to the bathing solution in the presence of histone H1 carrier. Amiloride subsequently added to the bath solution toward the end of the experiment. This representative patch contains, at least, five ENaC. Shown at top is a continuous trace. Shown below (left) at an expanded timescale are regions of the trace before (1. control; middle) and after (2. PIP_3; bottom) addition of exogenous phosphoinositide. Respective all-point histograms for the regions shown at an expanded timescale are to the right. All other conditions the same as Fig. 3 A.

(β2D; B) channels. $PI(3,4,5)P_3$ markedly increases P_o of ENaC-containing α2D. In contrast, exogenous $PI(3,4,5)P_3$ has little effect on the P_o of channels containing β2D.

Fig. 6 (A–D) summarizes the effects of exogenous $PI(3,4,5)P_3$ on ENaC P_o for wild-type channels and channels containing either the α2D, β2D, or γ2S mutant subunits. Effects on P_o were quantified in paired experiments similar to the representative experiments shown in Fig. 5. Channels containing all wild-type subunits and those containing the α2D mutant were fully responsive to $PI(3,4,5)P_3$. In contrast, those having either the β2D or γ2S mutant subunit failed to respond to $PI(3,4,5)P_3$. These results are consistent with those in Fig. 2. Also consistent are the results summarized in Fig. 6 (E–H).

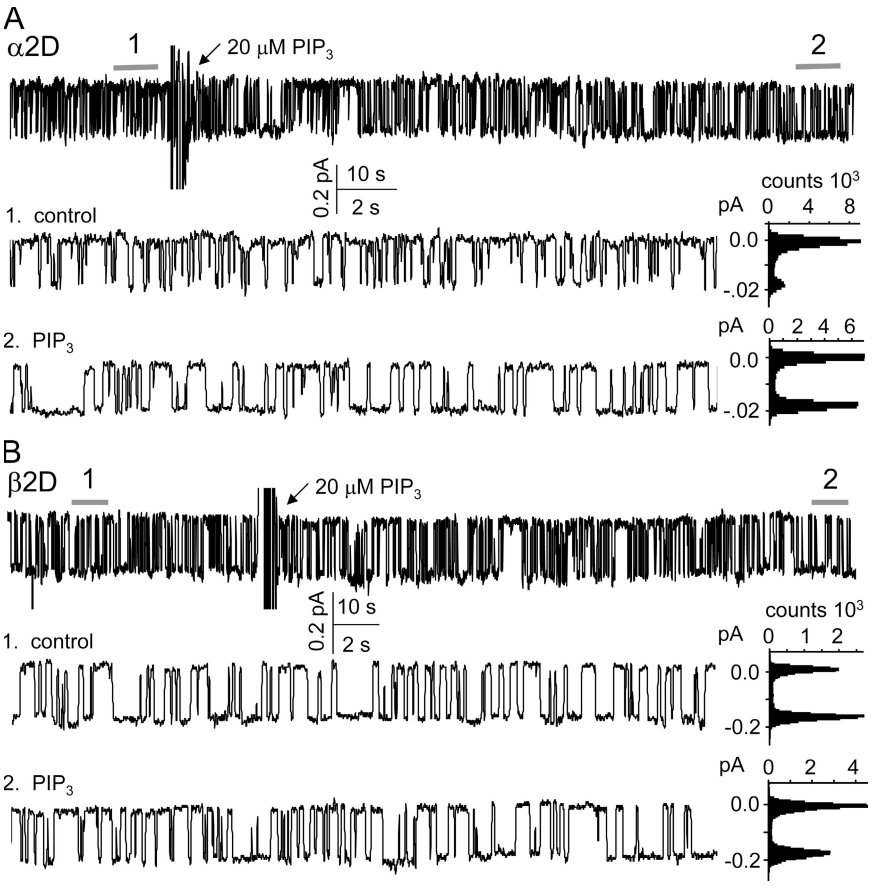

Figure 5. ENaC containing mutant α2D but not β2D subunits have a typical response to exogenous $PI(3,4,5)P_3$: an increase in P_o. (A) Representative current traces containing a single ENaC from excised, outside-out patches (V_p = 0 mV) from CHO cells expressing ENaC containing the α2D (A) and β2D (B) mutant subunits before and after addition of 20 μM $PI(3,4,5)P_3$. Shown at top are continuous traces. Shown below (left) at expanded timescales are regions of these traces before (1. control) and after (2. PIP_3) addition of phosphoinositide. Respective all-point histograms for the regions shown at an expanded timescale are to the right. All other conditions the same as Fig. 4.

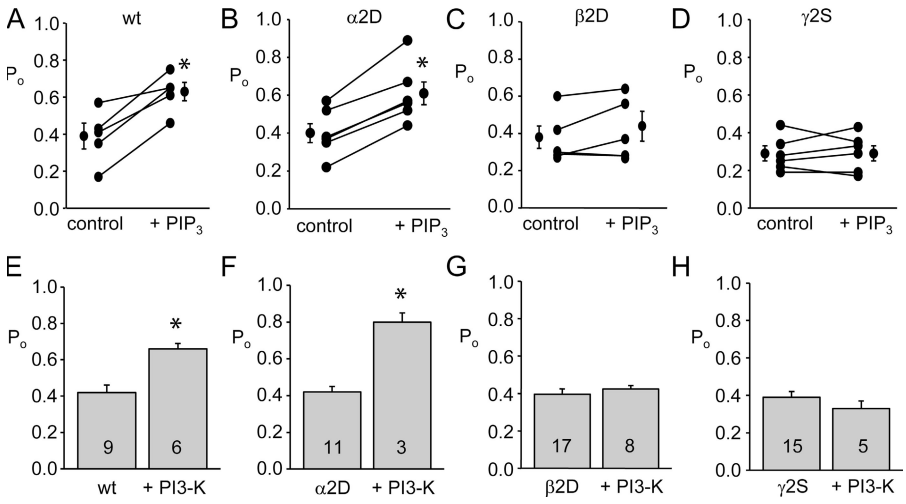

Figure 6. Positive-charged residues just following TM2 in β and γ subunits are necessary for PI3-K and $PI(3,4,5)P_3$-dependent increases in ENaC open probability. Summary graphs of the effects of $PI(3,4,5)P_3$ on P_o for recombinant ENaC expressed in CHO cells containing all three wild-type subunits (A) and single mutant subunits in the presence of the two other complementary wild-type subunits (B–D). Results are from paired excised, outside-out patch clamp experiments similar to those in Fig. 5. *, significantly greater compared with the absence of $PI(3,4,5)P_3$. Summary graphs of the effects on P_o of expressing recombinant ENaC in CHO cells in the absence and presence of constitutively active PI3-K. ENaC containing all three wild-type subunits (E) and single mutant subunits in the presence of the two other complementary wild-type subunits (F–H) were expressed. Results are from unpaired excised, outside-out patch clamp experiments similar to those in Fig. 3. *, significantly greater compared with the absence of PI3-K.

Shown here is P_o for wild-type channels and channels containing α2D, β2D, and γ2S mutant subunits in the absence and presence of coexpression of PI3-K. Open probability was quantified in unpaired experiments using excised, outside-out patches similar to those in Fig. 3. Channels containing all wild-type subunits and those containing α2D but not β2D or γ2S mutant subunits had significantly greater P_o in the presence of PI3-K. These results as a whole emphasize the importance of the conserved positive-charged residues in the regions just following TM2 in β- and γ-ENaC to regulation of P_o by PI3-K and its phosphoinositide products.

Conserved Positive-charged Residues at the Extreme N Terminus of β- and γ-ENaC Are Necessary for $PI(4,5)P_2$ Regulation of P_o

After identifying regions of ENaC critical to regulation by PI3-K and $PI(3,4,5)P_3$, we wondered if these regions played a role in $PI(4,5)P_2$ regulation. To begin addressing this question, we next quantified regulation of ENaC by chronic stimulation of PI(4)P5-K signaling. Our goal was to establish conditions favoring chronic elevations in $PI(4,5)P_2$. As with overexpression of PI3-K, we first quantified ENaC activity in response to coexpression with PI(4)P5-K in whole-cell voltage-clamp experiments monitoring changes in macroscopic, amiloride-sensitive currents. Fig. 7 reports the relative increase in activity in response to PI(4)P5-K for channels containing all wild-type subunits and those containing a single type of mutant subunit coexpressed with complementary wild-type subunits. Under these conditions, PI(4)P5-K increased the activity of all channels. We interpret this finding as meaning that either none of the regions probed here play a role in regulation by $PI(4,5)P_2$ or that a response to chronic elevations in $PI(4,5)P_2$ is complex, involving possible changes in either the number of channels in the membrane or channel P_o or both. In consideration of earlier work (Staruschenko et al., 2004b; Pochynyuk et al., 2006a; Pochynyuk et al., 2007a), we suggest that chronic elevations in $PI(4,5)P_2$ increase the number of ENaC in the membrane and that the regions mutated in the current study do not have a role in this regulation. If this is correct, then possible effects on P_o may have been masked during chronic elevation of $PI(4,5)P_2$. Other possibilities that are not necessarily mutually exclusive also exist. For instance, $PI(4,5)P_2$ could repress negative regulation of channel P_o. If resting $PI(4,5)P_2$ levels are saturating for this effect but not for effects on N, then disrupting the $PI(4,5)P_2$ regulatory site relevant to P_o would have little effect on basal activity and activity increases in response to chronic elevations in $PI(4,5)P_2$. With such a scenario, $PI(4,5)P_2$ effects on channel activity via P_o would only become apparent at lower, nonsaturating levels of the phosphoinositide.

Thus, we were not completely satisfied by this initial probing of sites within ENaC potentially important to direct regulation of the channel by $PI(4,5)P_2$. Since we and others have had previous success modulating ENaC activity and P_o by decreasing $PI(4,5)P_2$ levels (Ma et al., 2002; Yue et al., 2002; Kunzelmann et al., 2005; Tong and Stockand, 2005), we next turned to this approach. However, before performing these experiments in an expression system, we wanted to confirm that such regulation is observable for native ENaC in epithelial cells with the goal of using identical tools to manipulate $PI(4,5)P_2$ and possibly ENaC P_o in both systems. We and others have previously decreased $PI(4,5)P_2$ levels indirectly by pushing the equilibrium between tyrosine kinases and protein tyrosine phosphatases toward the prior

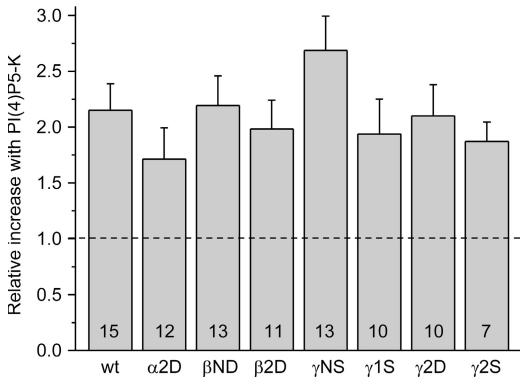

Figure 7. Mutant and wild-type ENaC have similar responses to coexpression with PI(4)P5-K. Summary graph of the relative increase in ENaC activity in the presence of coexpressed PI(4)P5-K for wild-type channels and channels containing a single type of mutant subunit expressed with complementary wild-type subunits. Activity of recombinant wild-type and mutant ENaC quantified in whole-cell voltage clamp experiments on CHO cells. All conditions the same as in Fig. 1 B. All channels had significantly greater activity in the presence of PI(4)P5-K and the relative increases in activity were not different compared with wild-type.

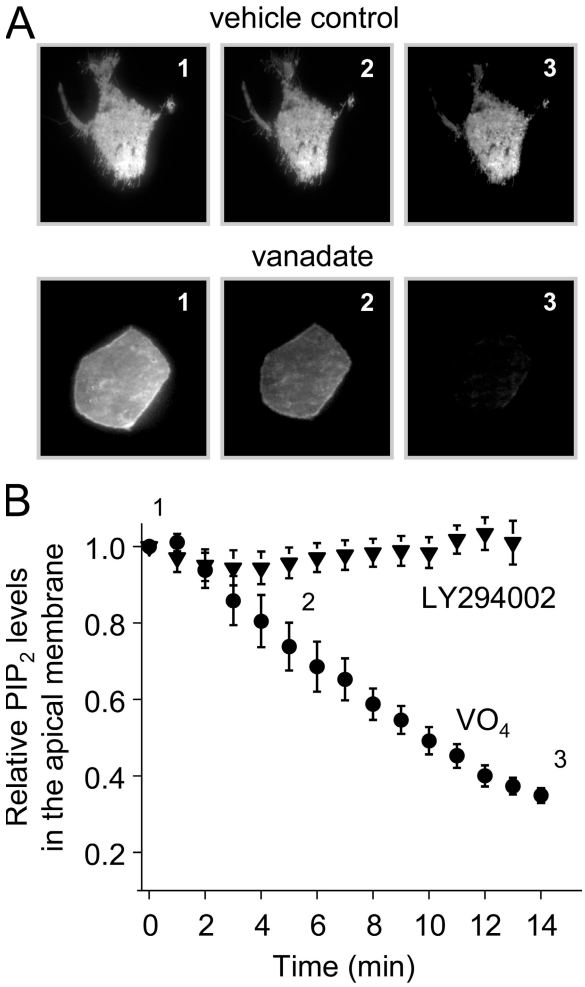

Figure 8. Vanadate decreases apical membrane PI(4,5)P_2 levels in mpkCCD$_{c14}$ principal cells within a confluent monolayer. (A) Fluorescence micrographs showing typical changes in apical membrane PI(4,5)P_2 levels in mpkCCD$_{c14}$ principal cells treated with vehicle (top) and 100 μM VO_4 (bottom). Cell are within confluent monolayers having high transepithelia resistances and avid Na^+ reabsorption. PI(4,5)P_2 was followed with the GFP-PLC-δ-PH reporter. Fluorescence emissions from the reporter in the apical membrane were optically isolated with TIRF microscopy. Cells are shown before (1) and 5 (2) and 15 (3) min after treatment. (B) Summary graph showing the time course of decrease in the relative levels of PI(4,5)P_2 within the apical membrane of mpkCCD$_{c14}$ cells in response to VO_4 (n = 5) and LY294002 (n = 9). Apical membrane PI(4,5)P_2 levels were quantified from experiments similar to the typical experiments shown in Fig. 8 A.

(Bezzerides et al., 2004; Tong and Stockand, 2005). This allows PLC-γ, a tyrosine kinase target, to predominate decreasing PI(4,5)P_2 levels.

Fig. 8 A shows fluorescence micrographs of emissions from a PI(4,5)P_2 reporter fused to eGFP in the apical membranes of mpkCCD$_{14}$ mouse principal cells within confluent epithelial monolayers before (1) and 5 (2) and 15 (3) min after addition of vehicle (top) and 100 μM vanadate (bottom). For these experiments, emissions from the apical membrane were optically isolated with TIRF microscopy. Only monolayers cultured in the presence of FBS and corticosteroids that exhibited robust Na^+ transport, thus containing active ENaC, were used. As is clear in this representative experiment and in the summary graph in Fig. 8 B, addition of vanadate rapidly decreases apical membrane PI(4,5)P_2 levels (n = 5). In contrast, PI(4,5)P_2 levels within the apical membrane were not influenced by the negative control of inhibiting PI3-K with LY294002 (50 μM; n = 9). Vanadate decreases PI(4,5)P_2 levels in CHO cells with a similar time course (Tong and Stockand, 2005).

As shown by the experiments in Fig. 9, decreasing PI(4,5)P_2 levels with vanadate decreases ENaC P_o in mpkCCD$_{14}$ principal cells. Shown in Fig. 9 A is a representative current trace from a cell-attached patch made on the apical membrane of an mpkCCD$_{c14}$ cell within a monolayer before and after addition of vanadate. This patch contains a single ENaC. Fig. 9 B shows the all points histograms associated with this channel before and after vanadate. The summary graph in Fig. 9 C of similar paired experiments demonstrates that decreasing PI(4,5)P_2 with vanadate significantly decreases P_o of native ENaC. In contrast, vehicle had no effect on P_o (0.29 ± 0.07 before and 0.27 ± 0.07 after; n = 4; unpublished data). A similar rapid decrease in ENaC P_o is observed in paired cell-attached patch clamp experiments when PI(4,5)P_2 levels are decreased with ATP activation of purinergic receptors (P_o = 0.32 ± 0.09 and 0.02 ± 0.01 before and after ATP; n = 6; unpublished data), and in an isolated, split-open rat collecting duct preparation when vanadate is used to decrease PI(4,5)P_2 levels (unpublished data).

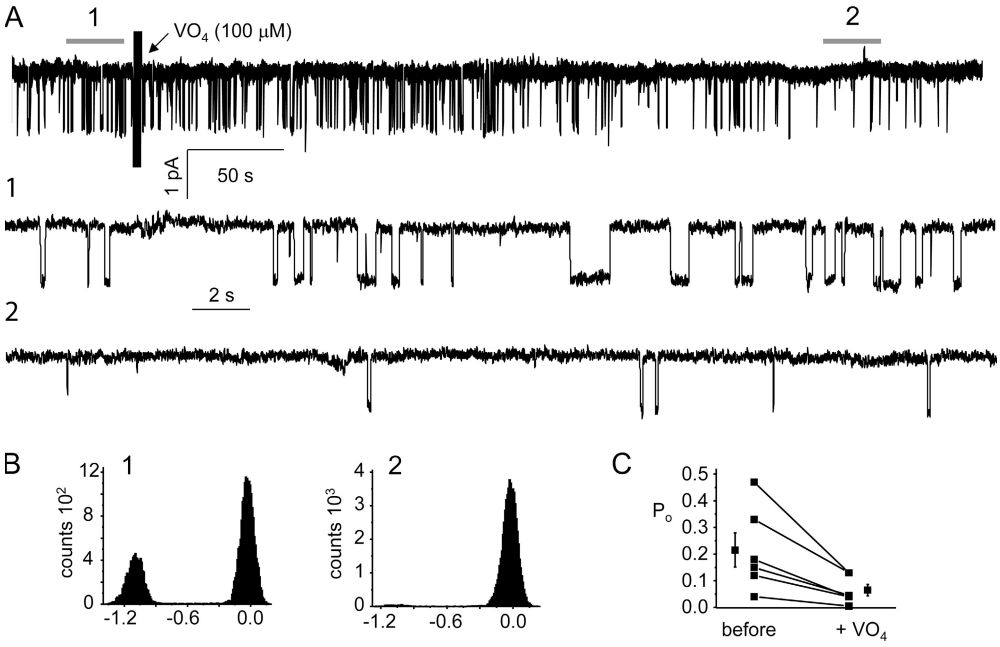

Figure 9. Decreases in ENaC open probability in mpkCCD$_{c14}$ principal cells treated with vanadate parallel decreases in apical membrane PI(4,5)P_2 levels. (A) Representative current trace of ENaC in a cell-attached patch ($-V_p$ = -60 mV) made on the apical membrane of a mpkCCD$_{c14}$ principal cell within a confluent monolayer before and after addition of vanadate. The major cation in the pipette solution was Li^+. Inward current is downwards. Shown at top is a continuous current trace. Shown below are portions of this trace before (1) and after vanadate (2) at an expanded timescale. Corresponding all-point histograms for these regions are shown in B. Results for decreases in ENaC P_o following treatment with vanadate from six such paired experiments are summarized in C. *, significantly less P_o compared with before addition of vanadate.

After confirming regulation of native ENaC in epithelial cells by manipulating PI(4,5)P_2 levels with vanadate, we tested the effects of this agent on the activity of wild-type and mutant ENaC expressed in CHO cells. The summary graph in Fig. 10 reports the relative decrease in activity for wild-type and mutant channels in response to vanadate. As expected, vanadate acutely decreased activity. Channels containing subunits with the N terminus of β-ENaC deleted (βND) or the conserved lysines within the N terminus of γ-ENaC neutralized to alanines (γNS) were resistant to the effects of vanadate, with the latter having significantly more activity in the presence of vanadate compared with wild-type channels. When the βND and γNS mutant subunits were incorporated into the same channel, decreasing PI(4,5)P_2 levels with vanadate had no effect on activity, demonstrating that these regions of ENaC, in particular, their conserved positive-charged residues, are critical to deceases in activity in response to a reduction of PI(4,5)P_2.

To better understand the molecular mechanism of action of PI(4,5)P_2 depletion in response to vanadate on ENaC, we studied this phenomena with single channel resolution. Fig. 11 shows representative current traces of ENaC in outside-out patches from CHO cells expressing recombinant channels containing all wild-type subunits (A) and γNS (B) mutant subunits before and after treatment with vanadate. As is clear in these representative experiments and in the corresponding summary graphs of similar paired experiments (Fig. 11 C = wt, D = α2D, and E = γNS), vanadate significantly and rapidly decreases the P_o of channels containing wild-type and α2D mutant subunits but not those containing the γ1S mutant subunit. These results are consistent with those in Fig. 10 and support a role for the conserved positive-charged residues in the N terminus of γ- and β-ENaC in the dynamic regulation of P_o by acute decreases in PI(4,5)P_2.

The direct effects of exogenous PI(4,5)P_2 on ENaC open probability were measured next in paired experiments using excised, inside-out patches. Results from these experiments are shown in Fig. 12. As expected, ENaC activity quickly decreases following patch excision. Such rundown is well documented for ENaC and several other channels in the excised, inside-out patch configuration. The cause of rundown remains unclear; however, it may be related to loss of a factor necessary/permissive for channel gating. Nevertheless, as documented by the representative current trace in Fig. 12 A and summarized in C, addition of 20 μM PI(4,5)P_2 to the intracellular face of wild-type ENaC quickly recovers activity. Channels containing γNS and βND mutant subunits, in contrast, do not respond to exogenous PI(4,5)P_2. Fig. 12 B contains a representative current trace for these channels, with D containing summarized data. The rapidity with which rundown wild-type channels recover activity in response to exogenous PI(4,5)P_2 in excised patches presumably inert with respect to trafficking is consistent with effects on P_o. It is important to note though that this also could reflect activation of previously quiescent/inactive channels. Moreover, possible (additional) effects on N likely are missed with these

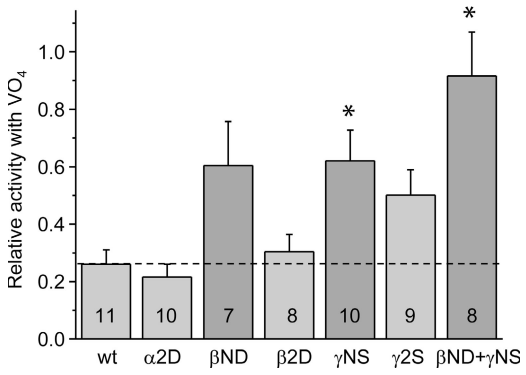

Figure 10. Positive-charged residues within the N termini of β and γ subunits are necessary for $PI(4,5)P_2$ regulation of ENaC activity. Summary graph of relative activity of recombinant wild-type and mutant ENaC following treatment with vanadate. Mutant channels contained, as indicated, one or two types of mutant subunits. Activity quantified in whole-cell voltage clamp experiments on CHO cells. All conditions the same as in Fig. 1 C. *, significantly smaller decrease in relative activity in response to vanadate compared with wild type using an ANOVA plus the Dunnett's subtest.

experimental conditions. Nevertheless, if one assumes that ENaC rundown does not exclusively result from loss of $PI(4,5)P_2$, then these findings agree with the VO_4 results made above and are consistent with regions in the extreme N termini of β- and γ-ENaC playing a role in regulation by $PI(4,5)P_2$.

DISCUSSION

We identify in this study regions of ENaC necessary for phosphoinositide regulation. The composition and position of these regions are consistent with them possibly playing a role in phosphoinositide binding. They contain multiple positive-charged residues conserved across all species. They are well positioned to influence channel gating. Our results are consistent with both $PI(3,4,5)P_3$ and $PI(4,5)P_2$ impacting ENaC open probability in a fast and dynamic manner. Increasing the former elevates ENaC open probability above basal levels, demonstrating that this phosphoiniositide is modulatory and that its effects are not saturated at rest. Chronic increases in $PI(4,5)P_2$, in contrast, appear to have little effect on ENaC gating at rest. However, acute decreases in $PI(4,5)P_2$ markedly reduce ENaC open probability. Being mindful of the limitations inherent to all patch clamp studies, these findings suggest to us that basal $PI(4,5)P_2$ levels may be functionally saturating with respect to modulation of ENaC in CHO cells and that resting levels of this phosphoinositide exert significant action on the channel. If correct, then $PI(4,5)P_2$ may be necessary for

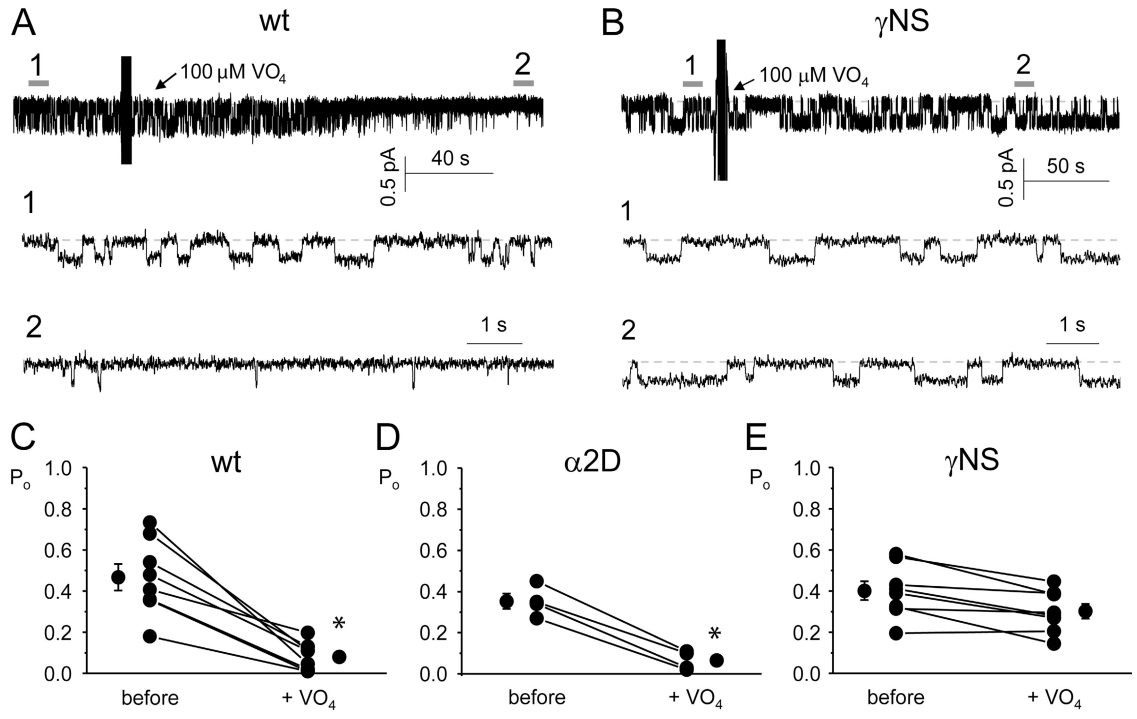

Figure 11. Positive-charged residues within the N terminus of γ-ENaC are critical for a response to decreases in membrane $PI(4,5)P_2$ levels. Representative current traces containing recombinant ENaC in excised, outside-out patches ($V_p = -60$ mV) from CHO cells expressing wild-type (A) and γNS (B) ENaC before and after addition of 100 μM VO_4. Shown at top are continuous traces. Shown below at expanded timescales are regions of these traces before (1) and after (2) vanadate. Summary graphs of the effects of vanadate on P_o for wild type (C; $n = 8$ with an average value of $N = 1.5 \pm 0.22$), α2D (D; $n = 4$ with an average value of $N = 2.25 \pm 0.45$), and γNS (E; $n = 8$ with an average value of $N = 2.3 \pm 0.33$) ENaC. *, significant decrease in P_o in response to VO_4.

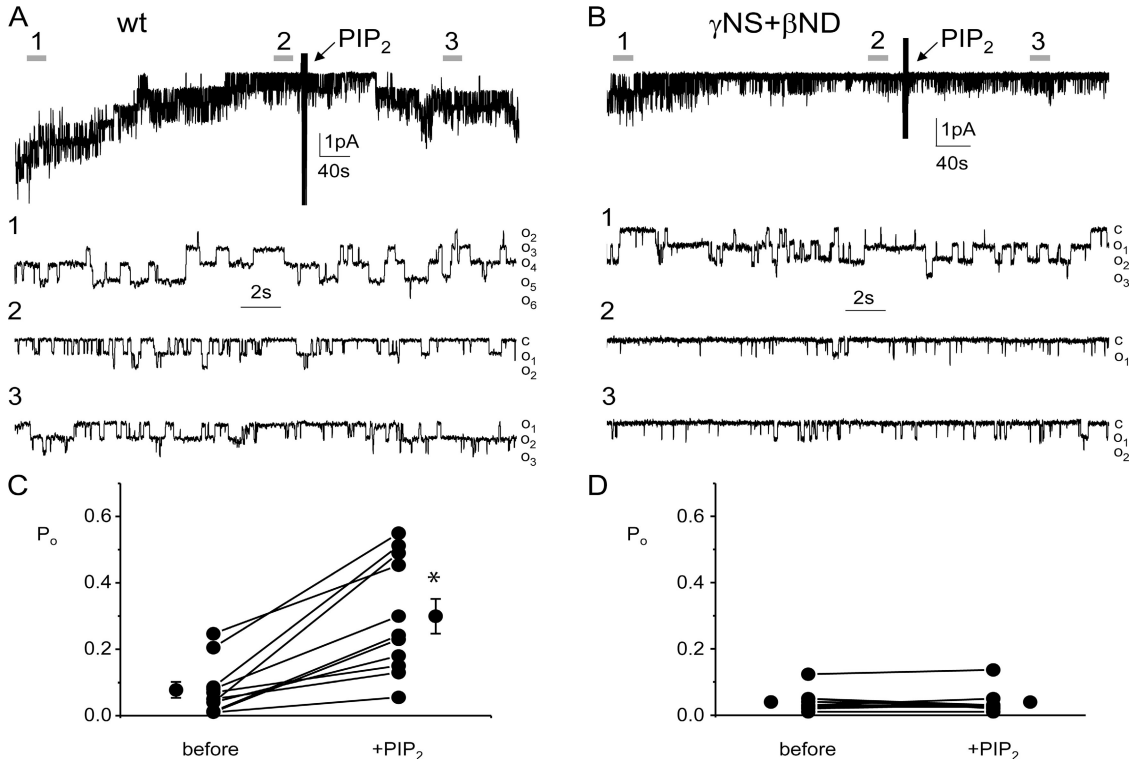

Figure 12. Positive-charged residues within the N termini of β- and γ-ENaC are necessary for $PI(4,5)P_2$ regulation of ENaC P_o. (A) Representative ENaC current traces from excised, inside-out patches ($-V_p = -60$ mV) made on CHO cells expressing wild-type (A) and γNS + βND (B) channels before and after addition of 20 μM $PI(4,5)P_2$. Shown at top are continuous traces. Shown below at expanded timescales are regions of these traces before rundown (1) and just before (2) and after (3) addition of $PI(4,5)P_2$. Respective summary graphs in C and D. (For both wt and mutant channels, $n = 11$ with average values of $N = 3.4 \pm 0.60$ and 2.0 ± 0.38, respectively. Two data points in the summary graph for wt channels were from traces containing six and eight channels.) *, vs. before $PI(4,5)P_2$.

normal ENaC gating in a manner similar to its actions on other ion channels, specifically Kir and TRPM; binding of $PI(4,5)P_2$ primes the channel to gate constitutively and in response to additional modulators (Huang et al., 1998; Zhang et al., 1999; Enkvetchakul et al., 2005; Ribalet et al., 2005, 2006; Rohacs et al., 2005; Nilius et al., 2006). We report here that the regions at the extreme N terminus of β- and γ-ENaC are critical to regulation by $PI(4,5)P_2$ but not $PI(3,4,5)P_3$. In contrast, the intracellular regions just following TM2 in β- and γ- but not α-ENaC are critical to regulation by $PI(3,4,5)P_3$ but not $PI(4,5)P_2$.

The Putative $PI(3,4,5)P_3$ Binding Site

Compared with ENaC, more is known about phosphoiniositide binding sites and their associated molecular mechanisms in other ion channels comprised of subunits having two transmembrane domains. The regions of β- and γ-ENaC that are necessary for $PI(3,4,5)P_3$ stimulation are very similar to the proposed phosphoinositide binding sites in all Kir channels (Zhang et al., 1999; Soom et al., 2001; Lopes et al., 2002; Ribalet et al., 2005; Ma et al., 2007). These contain several well-conserved positive-charged residues at the interface between a trans membrane domain involved in pore formation and possibly gating and the intracellular domains of the polypeptide. Neither the proposed phosphoinositide binding site in Kir channels nor that proposed here for $PI(3,4,5)P_3$ in β- and γ-ENaC subunits fits the classic examples of phosphoinositide binding sites, including PH, PX, and FYVE domains, well established in many signaling proteins (Lemmon, 2003). So, much remains unknown about how such putative binding sites within ion channels coordinate phosphoinositide binding. Nevertheless, phosphoinositide binding to ion channels, in general, is believed to involve electrostatic interactions between basic residues within the binding domain and anionic phosphate head groups of the phospholipid.

The Putative $PI(4,5)P_2$ Binding Site

As with the putative $PI(3,4,5)P_3$ binding sites in the C termini of β- and γ-ENaC, those identified in the extreme N termini of these subunits involved in $PI(4,5)P_2$ regulation contain several conserved basic residues, and are similar in composition to the proposed phosphoinositide binding sites in other channels. The site in the N terminus of γ-ENaC contains the [R/K]-$X_{3\text{-}11}$- [R/K]-X-[R/K]-[R/K] motif (where x is any amino acid) common to PH domains. A similar sequence is apparent in the phosphoinositide binding site in the C terminus of TRPM4 (Nilius et al., 2006). Thus, phosphoinositide binding to ion channels

may have more in common, then first suspected, with binding of these molecules to signaling proteins. Additional analysis of the specific charged residues in the N terminus of γ-ENaC involved in coordinating $PI(4,5)P_2$ will determine whether this is coincidental and may provide a framework on which to map other putative phosphoinositide binding sites within ion channels.

The putative $PI(4,5)P_2$ binding sites in ENaC at the extreme N termini in β- and γ-ENaC subunits are far removed from the proposed channel gate. This makes it difficult to predict mechanism of action. Nevertheless, it is possible that $PI(4,5)P_2$ binding to this region of the channel immobilizes a negative regulator of the channel, allowing normal gating. While several alternatives exist that cannot be excluded with the current dataset, we favor this interpretation of our results.

A major difference exists regarding $PI(4,5)P_2$ and $PI(3,4,5)P_3$ regulation of ENaC. This being that the effects of $PI(4,5)P_2$ appear saturating at rest and permissive for normal channel gating. Thus, we propose that occupation of the putative $PI(4,5)P_2$ binding site in some manner removes a negative regulation of the channel. This is consistent with the current results; depleting $PI(4,5)P_2$ rapidly decreases ENaC P_o and charge neutralization/deletion of key basic residues at the N termini of β- and γ-ENaC render the channel insensitive to $PI(4,5)P_2$ without affecting basal P_o. Thus, it appears that the basic residues in the N terminus of β- and γ-ENaC in some manner restrict ENaC opening and that $PI(4,5)P_2$ occupies these to counter this negative regulation.

This proposed mechanism shares features with phosphoinositide regulation of K_v channels (Oliver et al., 2004). For these latter channels, $PI(4,5)P_2$ binds and immobilizes the cytoplasmic inactivation ball by gluing it to the plasma membrane, resulting in relief of N-type inactivation. This is not to say that ENaC gating is controlled by voltage or a ball and chain mechanism, but rather that $PI(4,5)P_2$ occupies a negative regulator of gating. The position of this switch then is defined by $PI(4,5)P_2$ binding and removal of this region of the channel is equivalent to binding. In contrast, removal of the $PI(3,4,5)P_3$ binding site is not equivalent to phosphoinositide binding, and thus $PI(3,4,5)P_3$ binding does not relieve inhibition but rather is stimulatory.

An important finding of this study is that these distinct phosphoinositides require different regions of the channel in order to affect open probability and activity. This finding is important for it explains how a channel, such as ENaC, sensitive to, at least, two different phosphoinositides, is capable of responding in the proper manner to each. Moreover, it provides the framework to understand how dynamic stimulation of ENaC open probability by $PI(3,4,5)P_3$ is possible in the presence of a distinct phosphoinositide, $PI(4,5)P_2$, that is relatively more abundant and exerting simultaneous regulation that appears to be functionally saturated at rest.

We propose that like $PI(4,5)P_2$ interactions with Kir, interaction of this phosphoinositide with ENaC sets the stage for subsequent regulation of gating by other channel modulators. Thus, $PI(4,5)P_2$ binding to ENaC is permissive for the channel to gate at a constitutive level, which then can be further modified by additional factors to include $PI(3,4,5)P_3$ binding at a distinct site. Such regulation of ENaC by $PI(4,5)P_2$ and $PI(3,4,5)P_3$ would have many parallels with contemporary thinking about regulation of Kir channels by $PI(4,5)P_2$ plus ATP and βγ G-protein subunits (Xie et al., 2006; Ribalet et al., 2005; Zhang et al., 1999; Huang et al., 1998). (We note that the basic residues in the N terminus of γ-ENaC, and likely those in β-ENaC, involved in a $PI(4,5)P_2$ response are identical to those targeted for ubiquitinylation by Nedd4 ubiquitin ligases during down-regulation of channel activity (Staub et al., 1997). It will be interesting to determine whether these residues play a role in signaling convergence between $PI(4,5)P_2$ regulation of P_o and Nedd4 regulation of N.)

Concluding Thoughts

Similar to β and γ subunits, α-ENaC has several intracellular tracks containing clusters of basic residues that are reminiscent of proposed phosphoinositide binding sites in other channels. However, in contrast to the other two subunits, we find no role for α-ENaC in a response to phosphoinositides. It is not clear why this subunit would not have a role in this regulation, and it may have been missed. Similarly, it is not clear why deletion and charge neutralization of intracellular regions of the channel just preceding TM1 result in loss of function, and the current results cannot exclude a role for these or any other channel domain in regulation by phosphoinositides. What we can conclude is that distinct regions within β- and γ-ENaC bestow sensitivity to both $PI(4,5)P_2$ and $PI(3,4,5)P_3$, allowing the channel to differentially respond to these phosphoinositides.

This research was supported by the National Institutes of Health grants RO1DK59594 and R01DK070571, and the American Heart Association grant EIA 0640054N (to J.D. Stockand).

Lawrence G. Palmer served as editor.

Submitted: 10 April 2007
Accepted: 10 September 2007

REFERENCES

Abriel, H., J. Loffing, J.F. Rebhun, J.H. Pratt, L. Schild, J.D. Horisberger, D. Rotin, and O. Staub. 1999. Defective regulation of the epithelial Na^+ channel by Nedd4 in Liddle's syndrome. *J. Clin. Invest.* 103:667–673.

Alvarez de la Rosa, D., C.M. Canessa, G.K. Fyfe, and P. Zhang. 2000. Structure and regulation of amiloride-sensitive sodium channels. *Annu. Rev. Physiol.* 62:573–594.

Axelrod, D. 2001. Total internal reflection fluorescence microscopy in cell biology 23. *Traffic.* 2:764–774.

Bender, K., M.C. Wellner-Kienitz, and L. Pott. 2002. Transfection of a phosphatidyl-4-phosphate 5-kinase gene into rat atrial myocytes

removes inhibition of GIRK current by endothelin and α-adrenergic agonists. *FEBS Lett.* 529:356–360.

Benos, D.J., and B.A. Stanton. 1999. Functional domains within the degenerin/epithelial sodium channel (Deg/ENaC) superfamily of ion channels. *J. Physiol.* 520:631–644.

Bens, M., V. Vallet, F. Cluzeaud, L. Pascual-Letallec, A. Kahn, M.E. Rafestin-Oblin, B.C. Rossier, and A. Vandewalle. 1999. Corticosteroid-dependent sodium transport in a novel immortalized mouse collecting duct principal cell line. *J. Am. Soc. Nephrol.* 10:923–934.

Bezzerides, V.J., I.S. Ramsey, S. Kotecha, A. Greka, and D.E. Clapham. 2004. Rapid vesicular translocation and insertion of TRP channels. *Nat. Cell Biol.* 6:709–720.

Bian, J.S., A. Kagan, and T.V. McDonald. 2004. Molecular analysis of PIP2 regulation of HERG and IKr. *Am. J. Physiol. Heart Circ. Physiol.* 287:H2154–H2163.

Blazer-Yost, B.L., T.G. Paunescu, S.I. Helman, K.D. Lee, and C.J. Vlahos. 1999. Phosphoinositide 3-kinase is required for aldosterone-regulated sodium reabsorption. *Am. J. Physiol.* 277: C531–C536.

Bonny, O., and E. Hummler. 2000. Dysfunction of epithelial sodium transport: From human to mouse. *Kidney Int.* 57:1313–1318.

Booth, R.E., and J.D. Stockand. 2003. Targeted degradation of ENaC in response to PKC activation of the ERK1/2 cascade. *Am. J. Physiol. Renal Physiol.* 284:F938–F947.

Booth, R.E., Q. Tong, J. Medina, P.M. Snyder, P. Patel, and J.D. Stockand. 2003. A region directly following the second transmembrane domain in gamma ENaC is required for normal channel gating. *J. Biol. Chem.* 278:41367–41379.

Canessa, C.M., J.D. Horisberger, and B.C. Rossier. 1993. Epithelial sodium channel related to proteins involved in neurodegeneration. *Nature.* 361:467–470.

Canessa, C.M., L. Schild, G. Buell, B. Thorens, I. Gautschi, J.D. Horisberger, and B.C. Rossier. 1994. Amiloride-sensitive epithelial Na channel is made of three homologous subunits. *Nature.* 367:463–467.

Cukras, C.A., I. Jeliazkova, and C.G. Nichols. 2002a. Structural and functional determinants of conserved lipid interaction domains of inward rectifying Kir6.2 channels. *J. Gen. Physiol.* 119:581–591.

Cukras, C.A., I. Jeliazkova, and C.G. Nichols. 2002b. The role of NH2-terminal positive charges in the activity of inward rectifier KATP channels. *J. Gen. Physiol.* 120:437–446.

Donaldson, M.R., J.L. Jensen, M. Tristani-Firouzi, R. Tawil, S. Bendahhou, W.A. Suarez, A.M. Cobo, J.J. Poza, E. Behr, J. Wagstaff, et al. 2003. PIP2 binding residues of Kir2.1 are common targets of mutations causing Andersen syndrome. *Neurology.* 60:1811–1816.

Dong, K., L. Tang, G.G. Macgregor, and S.C. Hebert. 2002. Localization of the ATP/phosphatidylinositol 4,5 diphosphate-binding site to a 39-amino acid region of the carboxyl terminus of the ATP-regulated K^+ channel Kir1.1. *J. Biol. Chem.* 277:49366–49373.

Du, X., H. Zhang, C. Lopes, T. Mirshahi, T. Rohacs, and D.E. Logothetis. 2004. Characteristic interactions with phosphatidylinositol 4,5-bisphosphate determine regulation of kir channels by diverse modulators. *J. Biol. Chem.* 279:37271–37281.

Enkvetchakul, D., I. Jeliazkova, and C.G. Nichols. 2005. Direct modulation of K channel gating by membrane PIP2. *J. Biol. Chem.* 280:35785–35788.

Fyfe, G.K., and C.M. Canessa. 1998. Subunit composition determines the single channel kinetics of the epithelial sodium channel. *J. Gen. Physiol.* 112:423–432.

Gamper, N., and M.S. Shapiro. 2006. Exogenous expression of proteins in neurons using the biolistic particle delivery system. *Methods Mol. Biol.* 337:27–38.

Gamper, N., V. Reznikov, Y. Yamada, J. Yang, and M.S. Shapiro. 2004. Phosphatidylinositol 4,5-bisphosphate signals underlie receptor-specific Gq/11-mediated modulation of N-type Ca^{2+} channels. *J. Neurosci.* 24:10980–10992.

Garty, H., and L.G. Palmer. 1997. Epithelial sodium channels: function, structure, and regulation. *Physiol. Rev.* 77:359–396.

Haugh, J., F. Codazzi, M. Teruel, and T. Meyer. 2000. Spatial sensing in fibroblasts mediated by 3′ phosphoinositides. *J. Cell Biol.* 151:1269–1280.

Hilgemann, D., S. Feng, and C. Nasuhoglu. 2001. The complex and intriguing lives of PIP2 with ion channels and transporters. *Sci. STKE.* 2001:RE19.

Huang, C.-L., S. Feng, and D.W. Hilgemann. 1998. Direct activation of inward rectifier potassium channels by PIP2 and its stabilization by Gβγ. *Nature.* 391:803–806.

Hummler, E., and J.D. Horisberger. 1999. Genetic disorders of membrane transport. V. The epithelial sodium channel and its implication in human diseases. *Am. J. Physiol.* 276:G567–G571.

Kellenberger, S., and L. Schild. 2002. Epithelial sodium channel/degenerin family of ion channels: a variety of functions for a shared structure. *Physiol. Rev.* 82:735–767.

Kemendy, A.E., T.R. Kleyman, and D.C. Eaton. 1992. Aldosterone alters the open probability of amiloride-blockable sodium channels in A6 epithelia. *Am. J. Physiol.* 263:C825–C837.

Kristof, A., J. Marks-Konczalik, E. Billings, and J. Moss. 2003. Stimulation of signal transducer and activator of transcription-1 (STAT1)-dependent gene transcription by lipopolysaccharide and interferon-γ is regulated by mammalian target of rapamycin. *J. Biol. Chem.* 278:33637–33644.

Kunzelmann, K., T. Bachhuber, R. Regeer, D. Markovich, J. Sun, and R. Schreiber. 2005. Purinergic inhibition of the epithelial Na^+ transport via hydrolysis of PIP2. *FASEB J.* 19:142–143.

Lemmon, M.A. 2003. Phosphoinositide recognition domains. *Traffic.* 4:201–213.

Li, Y., N. Gamper, D.W. Hilgemann, and M.S. Shapiro. 2005. Regulation of Kv7 (KCNQ) K^+ channel open probability by phosphatidylinositol 4,5-bisphosphate. *J. Neurosci.* 25:9825–9835.

Lifton, R.P., A.G. Gharavi, and D.S. Geller. 2001. Molecular mechanisms of human hypertension. *Cell.* 104:545–556.

Lin, Y.W., C. MacMullen, A. Ganguly, C.A. Stanley, and S.L. Shyng. 2006. A novel KCNJ11 mutation associated with congenital hyperinsulinism reduces the intrinsic open probability of β-cell ATP-sensitive potassium channels. *J. Biol. Chem.* 281:3006–3012.

Lopes, C., H. Zhang, T. Rohacs, T. Jin, and D. Logothetis. 2002. Alterations in conserved Kir channel-PIP2 interactions underlie channelopathies. *Neuron.* 34:933–944.

Lopes, C.M., T. Rohacs, G. Czirjak, T. Balla, P. Enyedi, and D.E. Logothetis. 2005. PIP_2-hydrolysis underlies agonist-induced inhibition and regulates voltage-gating of 2-P domain K^+ channels. *J. Physiol.* 564:117–129.

Ma, D., X.D. Tang, T.B. Rogers, and P.A. Welling. 2007. An andersen-Tawil syndrome mutation in Kir2.1 (V302M) alters the G-loop cytoplasmic K^+ conduction pathway. *J. Biol. Chem.* 282:5781–5789.

Ma, H.P., S. Saxena, and D.G. Warnock. 2002. Anionic phospholipids regulate native and expressed epithelial sodium channel (ENaC). *J. Biol. Chem.* 277:7641–7644.

McNicholas, C.M., and C.M. Canessa. 1997. Diversity of channels generated by different combinations of epithelial sodium channel subunits. *J. Gen. Physiol.* 109:681–692.

Nilius, B., F. Mahieu, J. Prenen, A. Janssens, G. Owsianik, R. Vennekens, and T. Voets. 2006. The Ca^{2+}-activated cation channel TRPM4 is regulated by phosphatidylinositol 4,5-biphosphate. *EMBO J.* 25:467–478.

Oliver, D., C.C. Lien, M. Soom, T. Baukrowitz, P. Jonas, and B. Fakler. 2004. Functional conversion between A-type and delayed rectifier K^+ channels by membrane lipids. *Science.* 304:265–270.

Park, K.H., J. Piron, S. Dahimene, J. Merot, I. Baro, D. Escande, and G. Loussouarn. 2005. Impaired KCNQ1-KCNE1 and phosphatidylinositol-4,5-bisphosphate interaction underlies the long QT syndrome. *Circ. Res.* 96:730–739.

Pochynyuk, O., A. Staruschenko, Q. Tong, J. Medina, and J.D. Stockand. 2005. Identification of a functional phosphatidylinositol 3,4,5-trisphosphate binding site in the epithelial Na^+ channel. *J. Biol. Chem.* 280:37565–37571.

Pochynyuk, O., J. Medina, N. Gamper, H. Genth, J.D. Stockand, and A. Staruschenko. 2006a. Rapid translocation and insertion of the epithelial Na^+ channel in response to RhoA signaling. *J. Biol. Chem.* 281:26520–26527.

Pochynyuk, O., Q. Tong, A. Staruschenko, H.P. Ma, and J.D. Stockand. 2006b. Regulation of the epithelial Na^+ channel (ENaC) by phosphatidylinositides. *Am. J. Physiol. Renal Physiol.* 290:F949–F957.

Pochynyuk, O., A. Staruschenko, V. Bugaj, L. LaGrange, and J.D. Stockand. 2007a. Quantifying RhoA facilitated trafficking of ENaC towards the plasma membrane with TIRF-FRAP. *J. Biol. Chem.* 282:14576–14585.

Pochynyuk, O., Q. Tong, A. Staruschenko, and J.D. Stockand. 2007b. Binding and direct activation of the epithelial Na^+ channel (ENaC) by phosphatidylinositides. *J. Physiol.* 580:365–372.

Prescott, E., and D. Julius. 2003. A modular PIP2 binding site as a determinant of capsaicin receptor sensititivity. *Science.* 300:1284–1288.

Record, R.D., L.L. Froelich, C.J. Vlahos, and B.L. Blazer-Yost. 1998. Phosphatidylinositol 3-kinase activation is required for insulin-stimulated sodium transport in A6 cells. *Am. J. Physiol.* 274: E611–E617.

Ribalet, B., S.A. John, L.H. Xie, and J.N. Weiss. 2005. Regulation of the ATP-sensitive K channel Kir6.2 by ATP and PIP(2). *J. Mol. Cell. Cardiol.* 39:71–77.

Ribalet, B., S.A. John, L.H. Xie, and J.N. Weiss. 2006. ATP-sensitive K^+ channels: regulation of bursting by the sulphonylurea receptor, PIP2 and regions of Kir6.2. *J. Physiol.* 571:303–317.

Rohacs, T., C. Lopes, T. Jin, P. Ramdya, Z. Molnar, and D. Logothetis. 2003. Specificity of activation by phosphoinositides determines lipid regulation of Kir channels. *Proc. Natl. Acad. Sci. USA.* 100:745–750.

Rohacs, T., C.M. Lopes, I. Michailidis, and D.E. Logothetis. 2005. PI(4,5)P2 regulates the activation and desensitization of TRPM8 channels through the TRP domain. *Nat. Neurosci.* 8:626–634.

Shyng, S.L., C.A. Cukras, J. Harwood, and C.G. Nichols. 2000. Structural determinants of PIP(2) regulation of inward rectifier K(ATP) channels. *J. Gen. Physiol.* 116:599–608.

Snyder, P.M., F.J. McDonald, J.B. Stokes, and M.J. Welsh. 1994. Membrane topology of the amiloride-sensitive epithelial sodium channel. *J. Biol. Chem.* 269:24379–24383.

Snyder, P.M., M.P. Price, F.J. McDonald, C.M. Adams, K.A. Volk, B.G. Zeiher, J.B. Stokes, and M.J. Welsh. 1995. Mechanism by which Liddle's syndrome mutations increase activity of a human epithelial Na^+ channel. *Cell.* 83:969–978.

Soom, M., R. Schonherr, Y. Kubo, C. Kirsch, R. Klinger, and S.H. Heinemann. 2001. Multiple PIP2 binding sites in Kir2.1 inwardly rectifying potassium channels. *FEBS Lett.* 490:49–53.

Staruschenko, A., J.L. Medina, P. Patel, M.S. Shapiro, R.E. Booth, and J.D. Stockand. 2004a. Fluorescence resonance energy transfer analysis of subunit stoichiometry of the epithelial Na^+ channel. *J. Biol. Chem.* 279:27729–27734.

Staruschenko, A., A. Nichols, J.L. Medina, P. Camacho, N.N. Zheleznova, and J.D. Stockand. 2004b. Rho small GTPases activate the epithelial Na^+ channel. *J. Biol. Chem.* 279:49989–49994.

Staruschenko, A., P. Patel, Q. Tong, J.L. Medina, and J.D. Stockand. 2004c. Ras activates the epithelial Na^+ channel through phosphoinositide 3-OH kinase signaling. *J. Biol. Chem.* 279:37771–37778.

Staruschenko, A., E. Adams, R.E. Booth, and J.D. Stockand. 2005. Epithelial Na^+ channel subunit stoichiometry. *Biophys. J.* 88:3966–3975.

Staub, O., I. Gautschi, T. Ishikawa, K. Breitschopf, A. Ciechanover, L. Schild, and D. Rotin. 1997. Regulation of stability and function of the epithelial Na^+ channel (ENaC) by ubiquitination. *EMBO J.* 16:6325–6336.

Steyer, J.A., and W. Almers. 2001. A real-time view of life within 100 nm of the plasma membrane. *Nat. Rev. Mol. Cell Biol.* 2:268–275.

Stockand, J.D. 2002. New ideas about aldosterone signaling in epithelia. *Am. J. Physiol. Renal Physiol.* 282:F559–F576.

Taraska, J.W., D. Perrais, M. Ohara-Imaizumi, S. Nagamatsu, and W. Almers. 2003. Secretory granules are recaptured largely intact after stimulated exocytosis in cultured endocrine cells. *Proc. Natl. Acad. Sci. USA.* 100:2070–2075.

Tong, Q., and J.D. Stockand. 2005. Receptor tyrosine kinases mediate epithelial Na^+ channel inhibition by epidermal growth factor. *Am. J. Physiol. Renal Physiol.* 288:F150–F161.

Tong, Q., R.E. Booth, R.T. Worrell, and J.D. Stockand. 2004a. Regulation of Na^+ transport by aldosterone: signaling convergence and cross talk between the PI3-K and MAPK1/2 cascades. *Am. J. Physiol. Renal Physiol.* 286:F1232–F1238.

Tong, Q., N. Gamper, J.L. Medina, M.S. Shapiro, and J.D. Stockand. 2004b. Direct activation of the epithelial Na^+ channel by phosphatidylinositol 3,4,5-trisphosphate and phosphatidylinositol 3,4-bisphosphate produced by phosphoinositide 3-OH kinase. *J. Biol. Chem.* 279:22654–22663.

Verrey, F. 1995. Transcriptional control of sodium transport in tight epithelial by adrenal steroids. *J. Membr. Biol.* 144:93–110.

Verrey, F. 1999. Early aldosterone action: toward filling the gap between transcription and transport. *Am. J. Physiol.* 277:F319–F327.

Voets, T., and B. Nilius. 2007. Modulation of TRPs by PIPs. *J. Physiol.* 582:939–944.

Wang, J., P. Barbry, A.C. Maiyar, D.J. Rozansky, A. Bhargava, M. Leong, G.L. Firestone, and D. Pearce. 2001. SGK integrates insulin and mineralocorticoid regulation of epithelial sodium transport. *Am. J. Physiol. Renal Physiol.* 280:F303–F313.

Wu, L., C.S. Bauer, X.G. Zhen, C. Xie, and J. Yang. 2002. Dual regulation of voltage-gated calcium channels by PtdIns(4,5)P2. *Nature.* 419:947–952.

Xie, L. H., S. A. John, B. Ribalet, and J. N. Weiss. 2006. Activation of inwardly rectifying potassium (Kir) channels by phosphatidylinositol-4,5-bisphosphate (PIP(2)): interaction with other regulatory ligands. *Prog. Biophys. Mol. Biol.* 94:320–335.

Yuan, W., A. Burkhalter, and J.M. Nerbonne. 2005. Functional role of the fast transient outward K^+ current IA in pyramidal neurons in (rat) primary visual cortex. *J. Neurosci.* 25:9185–9194.

Yue, G., B. Malik, G. Yue, and D.C. Eaton. 2002. Phosphatidylinositol 4,5-bisphosphate (PIP2) stimulates epithelial sodium channel activity in A6 cells. *J. Biol. Chem.* 277:11965–11969.

Zhang, H., C. He, X. Yan, T. Mirshahj, and D. Logothetis. 1999. Activation of inwardly rectifying K channels by distinct PtdIns(4,5)P2 interactions. *Nat. Cell Biol.* 1:183–188.